USGS
science for a changing world

U.S. Department of the Interior
U.S. Geological Survey

Open-File Report 2018–1158
Sheet 1 of 3

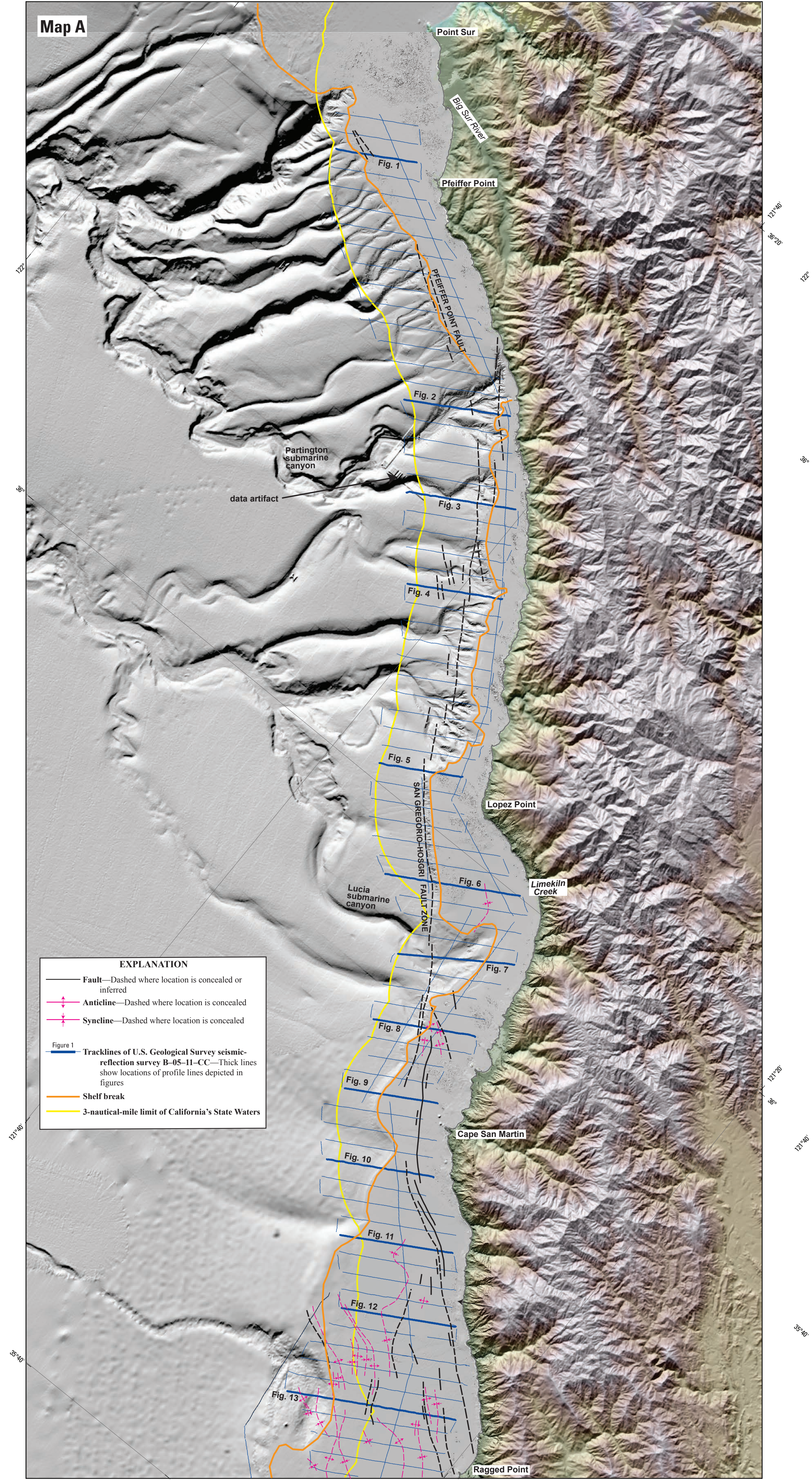

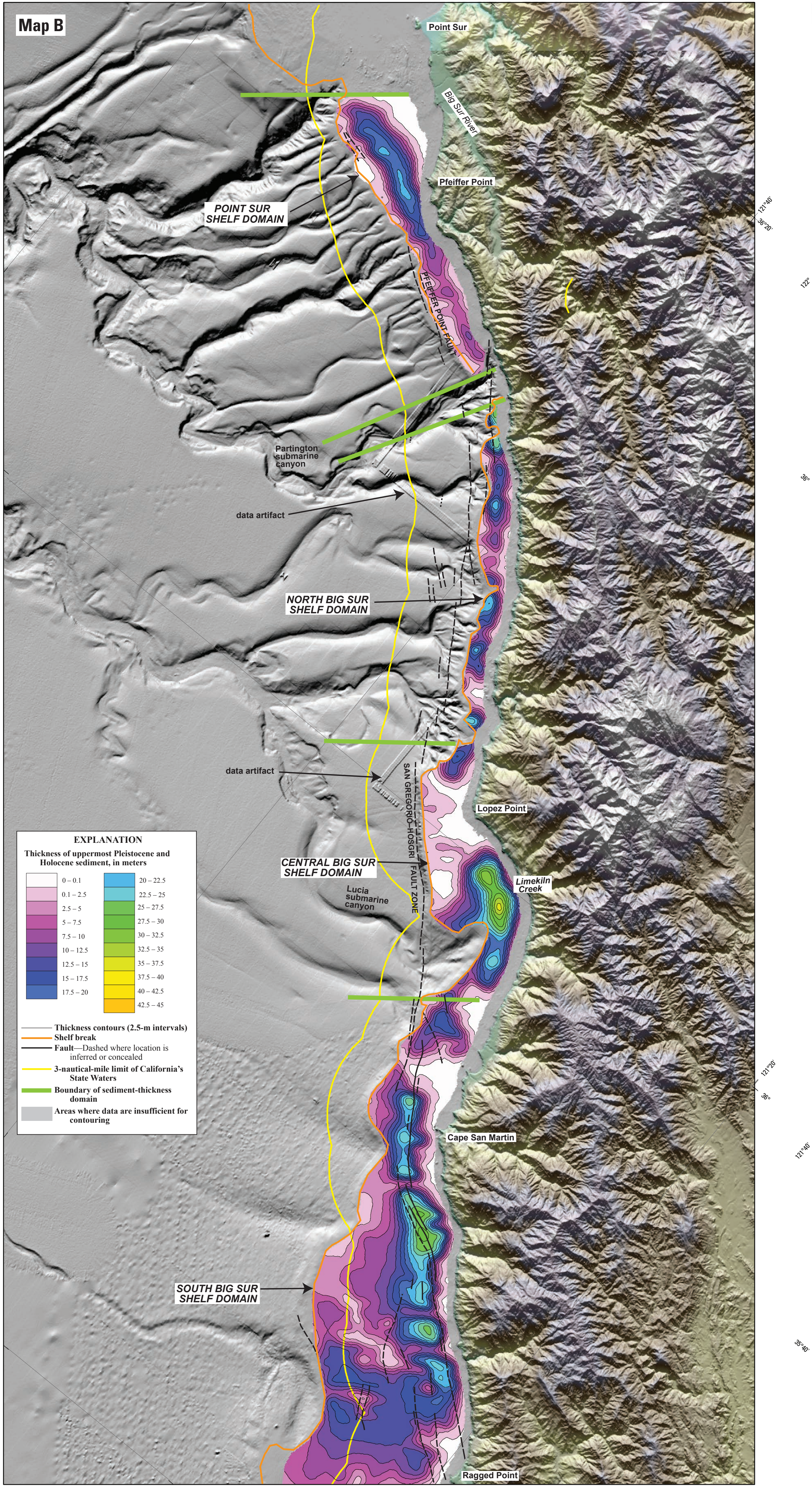

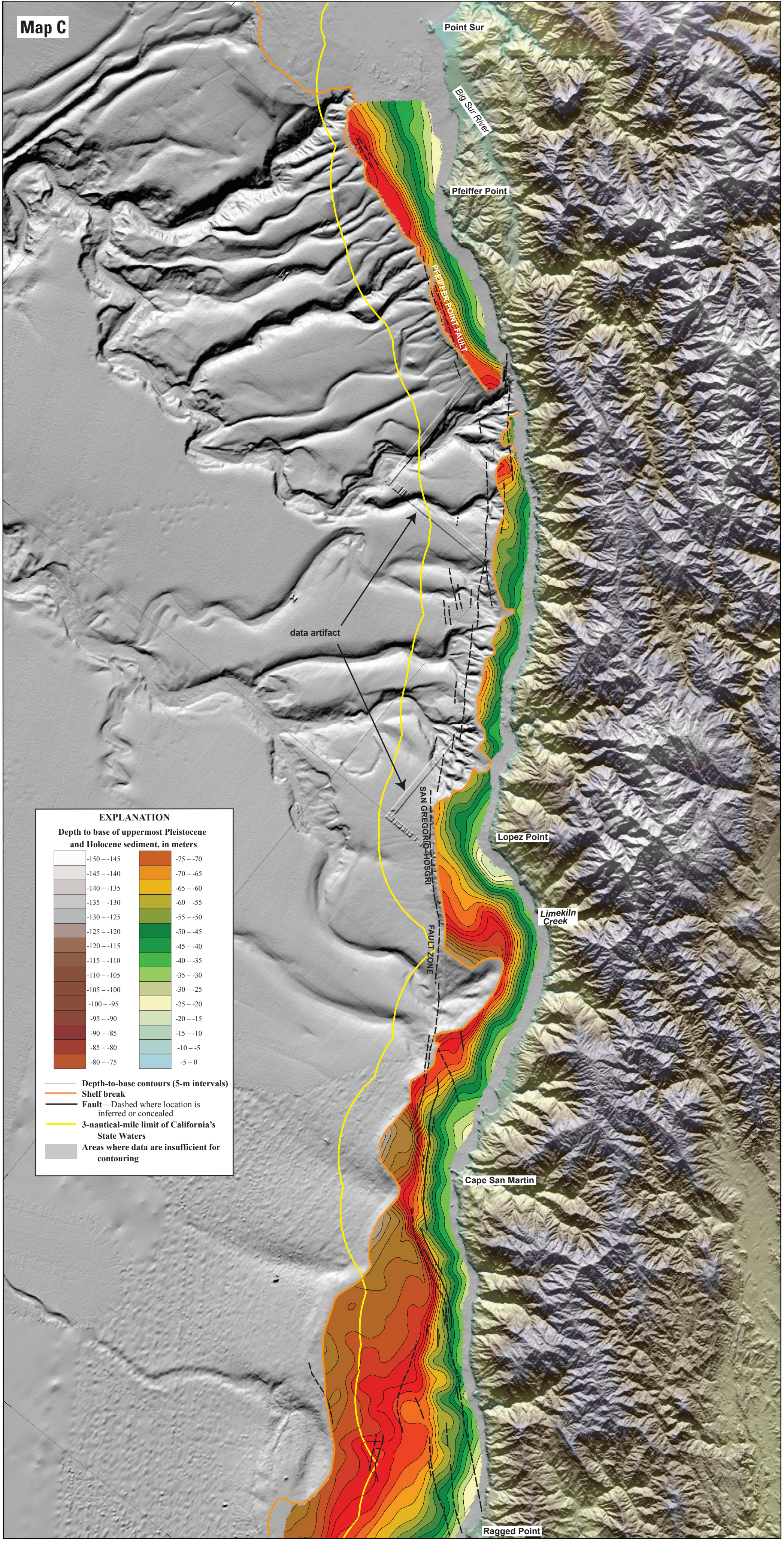

NOT INTENDED FOR NAVIGATIONAL USE

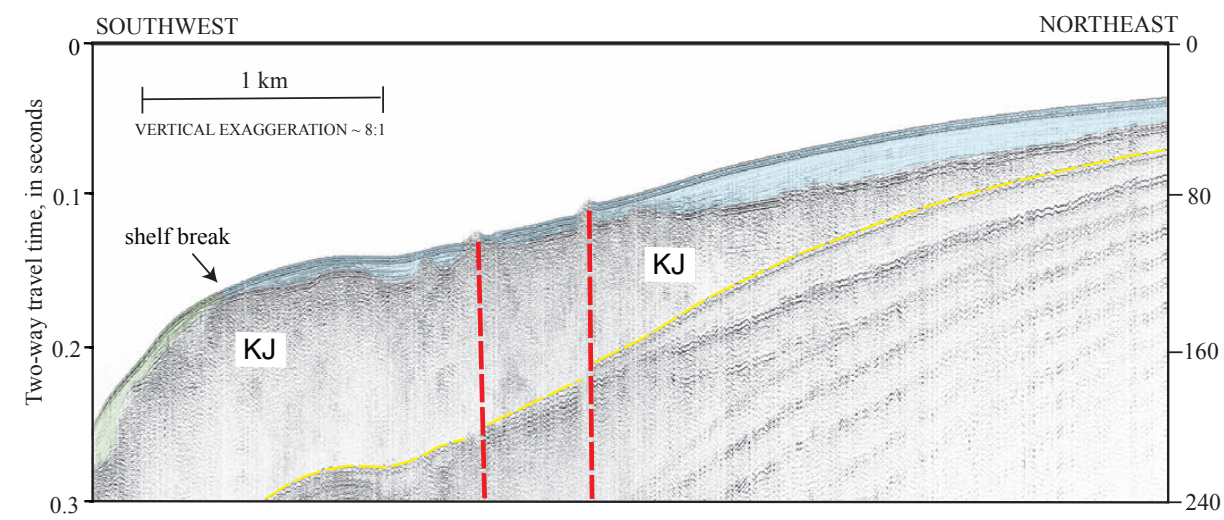

Figure 1. USGS high-resolution minisparker seismic-reflection profile BSS–01 (collected in 2011 on survey B–05–11–CC), which crosses shelf on west flank of Pfeiffer Point; see Map A for location. Dashed red lines show faults. Blue shading shows inferred uppermost Pleistocene and Holocene strata, deposited since last sea-level lowstand (Last Glacial Maximum) about 21,000 years ago. Green shading shows Quaternary slope deposits. 'KJ,' rocks of the Jurassic and Cretaceous Franciscan Complex. Dashed yellow line is seafloor multiple (echo of seafloor reflector).

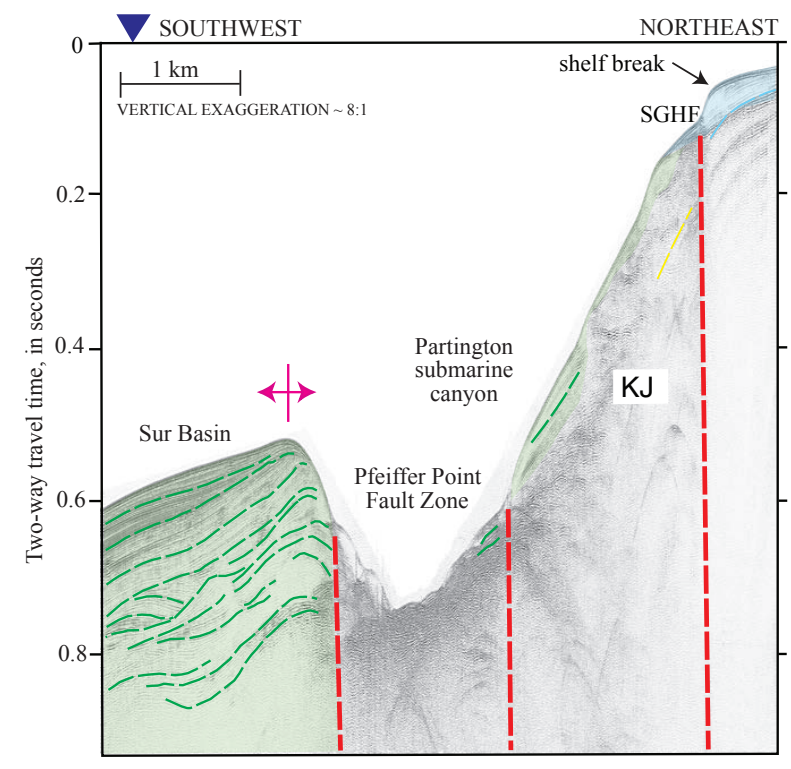

Figure 2. USGS high-resolution minisparker seismic-reflection profile BSS–24 (collected in 2011 on survey B–05–11–CC), which crosses informally named Partington submarine canyon southeast of Pfeiffer Point; see Map A for location. Dashed red lines show faults, including San Gregorio–Hosgri Fault (SGHF) and Pfeiffer Point Fault Zone. Magenta symbol shows anticline axis. Blue shading shows inferred uppermost Pleistocene and Holocene strata, deposited since last sea-level lowstand about 21,000 years ago. Green shading shows Quaternary slope deposits. 'KJ,' rocks of the Jurassic and Cretaceous Franciscan Complex. Dashed green lines highlight continuous reflections (not intended to show correlations across faults). Dashed yellow line is seafloor multiple (echo of seafloor reflector). Purple triangle shows approximate location of California's State Waters limit (yellow line on Maps A, B, C).

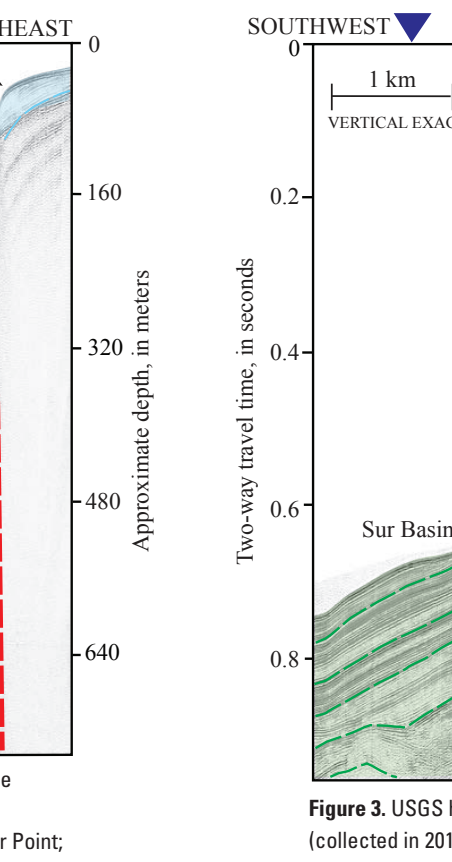

Figure 3. USGS high-resolution minisparker seismic-reflection profile BSS–32 (collected in 2011 on survey B–05–11–CC), which crosses shelf southeast of Pfeiffer Point; see Map A for location. Dashed red lines show faults, including San Gregorio–Hosgri Fault Zone (SGHF). Blue shading shows inferred uppermost Pleistocene and Holocene strata, deposited since last sea-level lowstand about 21,000 years ago. Green shading shows Quaternary slope deposits. 'KJ,' rocks of the Jurassic and Cretaceous Franciscan Complex. Dashed green lines highlight continuous reflections (not intended to show correlations across faults). Dashed yellow lines are seafloor multiples (echoes of seafloor reflector). Purple triangle shows approximate location of California's State Waters limit (yellow line on Maps A, B, C).

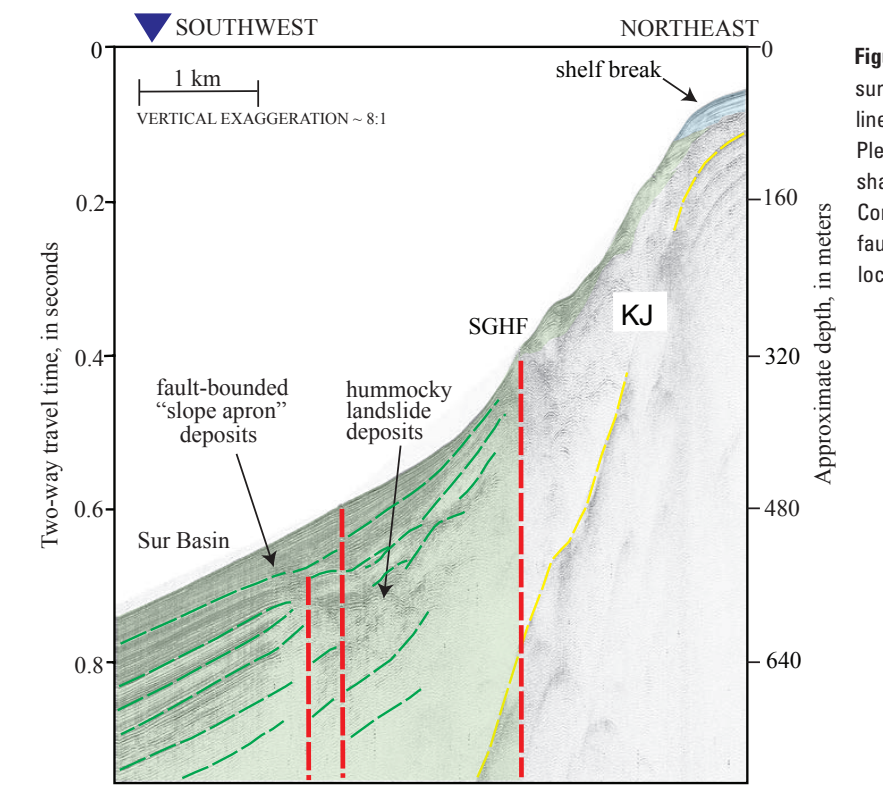

Figure 4 (left). USGS high-resolution minisparker seismic-reflection profile BSS–41 (collected in 2011 on survey B–05–11–CC), which crosses shelf northwest of Lopez Point; see Map A for location. Dashed red lines show faults, including San Gregorio–Hosgri Fault (SGHF). Blue shading shows inferred uppermost Pleistocene and Holocene strata, deposited since last sea-level lowstand about 21,000 years ago. Green shading shows Quaternary slope deposits. 'KJ,' rocks of the Jurassic and Cretaceous Franciscan Complex. Dashed green lines highlight continuous reflections (not intended to show correlations across faults). Dashed yellow lines are seafloor multiples (echoes of seafloor reflector). Purple triangle shows location of California's State Waters limit (yellow line on Maps A, B, C).

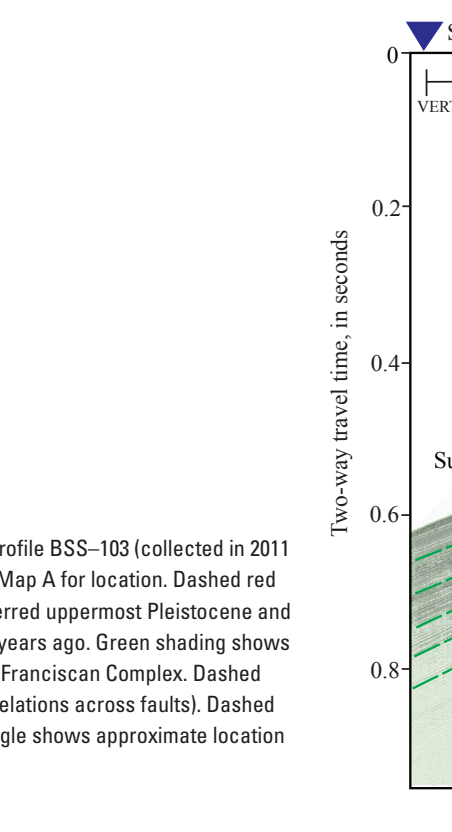

Figure 5 (right). USGS high-resolution minisparker seismic-reflection profile BSS–103 (collected in 2011 on survey B–05–11–CC), which crosses shelf west of Lopez Point; see Map A for location. Dashed red line shows San Gregorio–Hosgri Fault (SGHF). Blue shading shows inferred uppermost Pleistocene and Holocene strata, deposited since last sea-level lowstand about 21,000 years ago. Green shading shows Quaternary slope deposits. 'KJ,' rocks of the Jurassic and Cretaceous Franciscan Complex. Dashed green lines highlight continuous reflections (not intended to show correlations across faults). Dashed yellow line is seafloor multiple (echo of seafloor reflector). Purple triangle shows approximate location of California's State Waters limit (yellow line on Maps A, B, C).

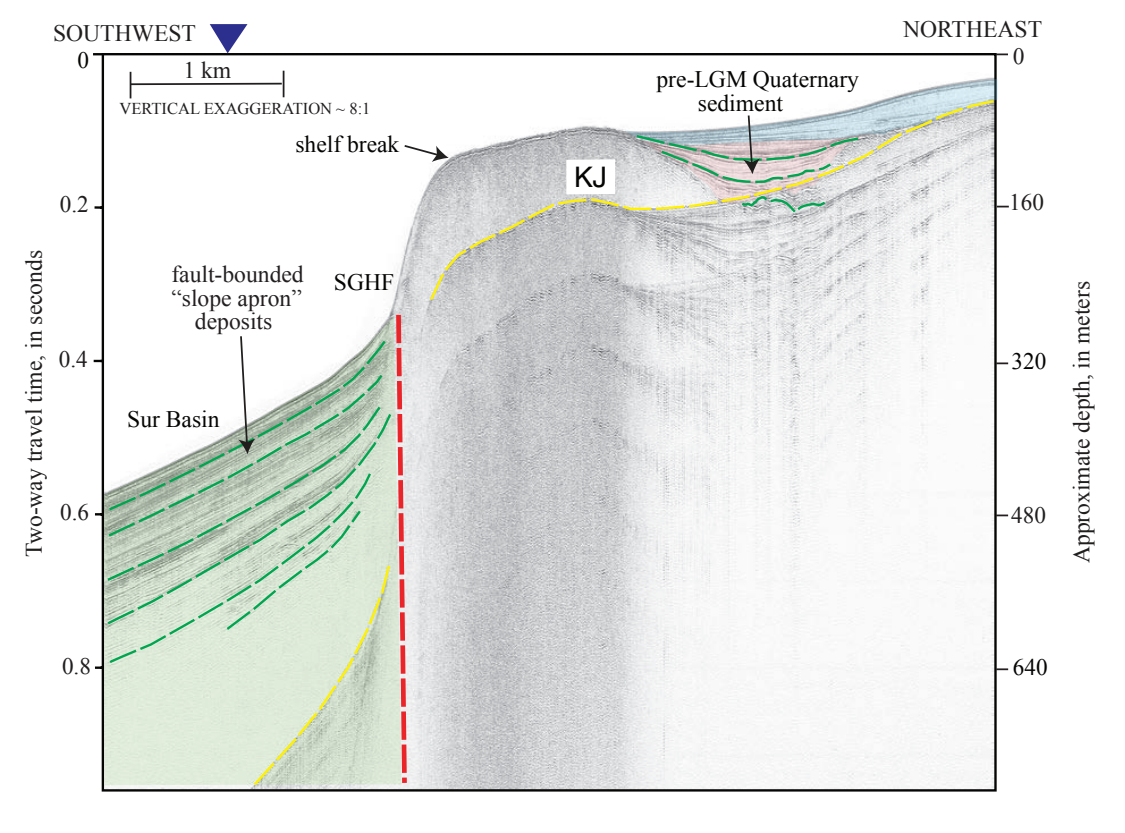

Figure 6 (left). USGS high-resolution minisparker seismic-reflection profile BSS–114 (collected in 2011 on survey B–05–11–CC), which crosses shelf south of Lopez Point; see Map A for location. Dashed red line shows San Gregorio–Hosgri Fault (SGHF). Blue shading shows inferred uppermost Pleistocene and Holocene strata, deposited since last sea-level lowstand (Last Glacial Maximum, LGM), about 21,000 years ago. Pink shading shows pre-LGM Quaternary sediment. Green shading shows Quaternary slope deposits. 'KJ,' rocks of the Jurassic and Cretaceous Franciscan Complex. Dashed green lines highlight continuous reflections (not intended to show correlations across faults). Dashed yellow lines are seafloor multiples (echoes of seafloor reflector). Purple triangle shows approximate location of California's State Waters limit (yellow line on Maps A, B, C).

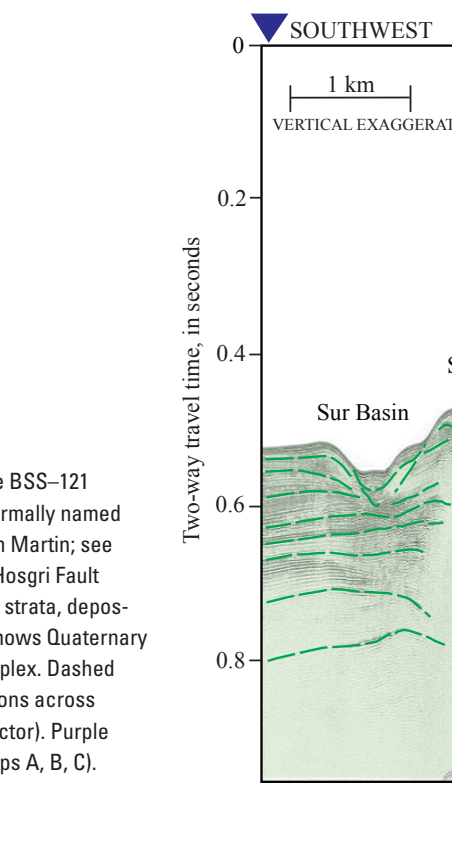

Figure 7 (right). USGS high-resolution minisparker seismic-reflection profile BSS–121 (collected in 2011 on survey B–05–11–CC), which crosses upper part of informally named Lucia submarine canyon, about midway between Lopez Point and Cape San Martin; see Map A for location. Dashed red lines show faults, including San Gregorio–Hosgri Fault (SGHF). Blue shading shows inferred uppermost Pleistocene and Holocene strata, deposited since last sea-level lowstand about 21,000 years ago. Green shading shows Quaternary slope deposits. 'KJ,' rocks of the Jurassic and Cretaceous Franciscan Complex. Dashed green lines highlight continuous reflections (not intended to show correlations across faults). Dashed yellow lines are seafloor multiples (echoes of seafloor reflector). Purple triangle shows location of California's State Waters limit (yellow line on Maps A, B, C).

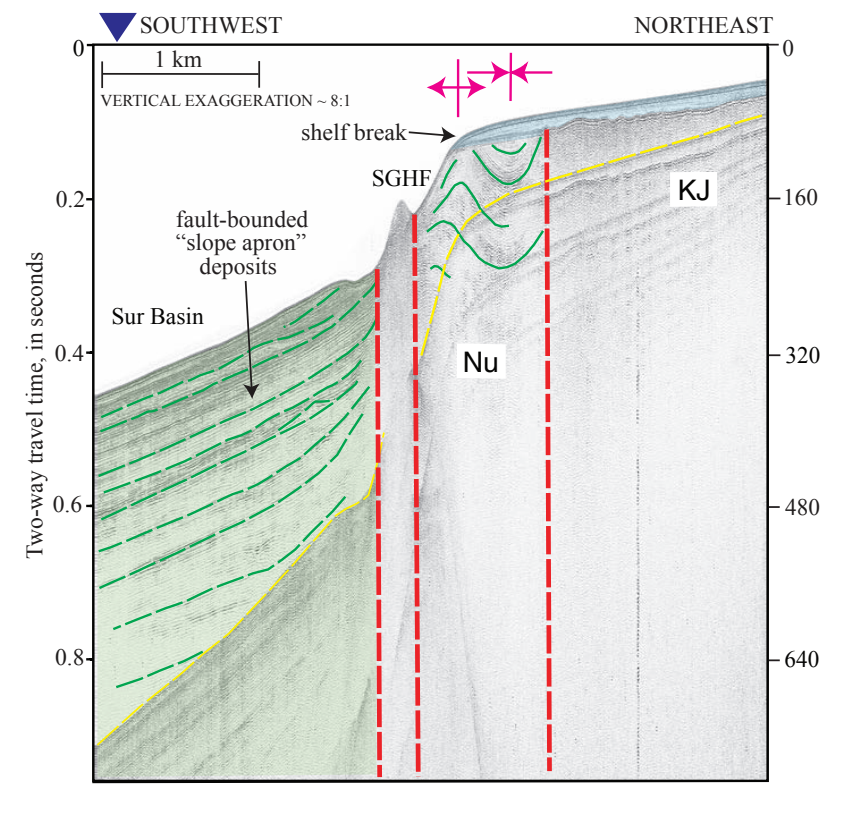

Figure 8 (left). USGS high-resolution minisparker seismic-reflection profile BSS–133 (collected in 2011 on survey B–05–11–CC), which crosses shelf northwest of Cape San Martin; see Map A for location. Dashed red lines show faults, including strands of San Gregorio–Hosgri Fault Zone (SGHF). Magenta symbols show fold axes (diverging arrows, anticline; converging arrows, syncline). Blue shading shows inferred uppermost Pleistocene and Holocene strata, deposited since last sea-level lowstand about 21,000 years ago. Green shading shows Quaternary slope deposits. 'Nu,' undivided Neogene strata; 'KJ,' rocks of the Jurassic and Cretaceous Franciscan Complex. Dashed green lines highlight continuous reflections (not intended to show correlations across faults). Dashed yellow lines are seafloor multiples (echoes of seafloor reflector). Purple triangle shows approximate location of California's State Waters limit (yellow line on Maps A, B, C).

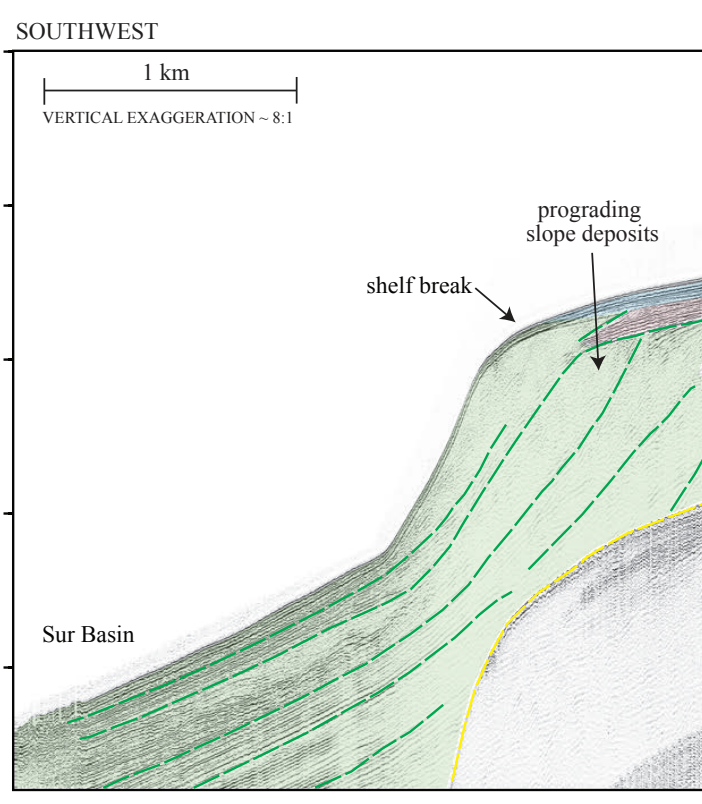

Figure 9 (right). USGS high-resolution minisparker seismic-reflection profile BSS–126 (collected in 2011 on survey B–05–11–CC), which crosses shelf west of Cape San Martin; see Map A for location. Dashed red lines show strands of San Gregorio–Hosgri Fault Zone (SGHF). Blue shading shows inferred uppermost Pleistocene and Holocene strata, deposited since last sea-level lowstand (Last Glacial Maximum, LGM), about 21,000 years ago. Pink shading shows pre-LGM Quaternary sediment. Green shading shows Quaternary slope deposits. 'KJ,' rocks of the Jurassic and Cretaceous Franciscan Complex. Dashed green lines highlight continuous reflections (not intended to show correlations across faults). Dashed yellow line is seafloor multiple (echo of seafloor reflector).

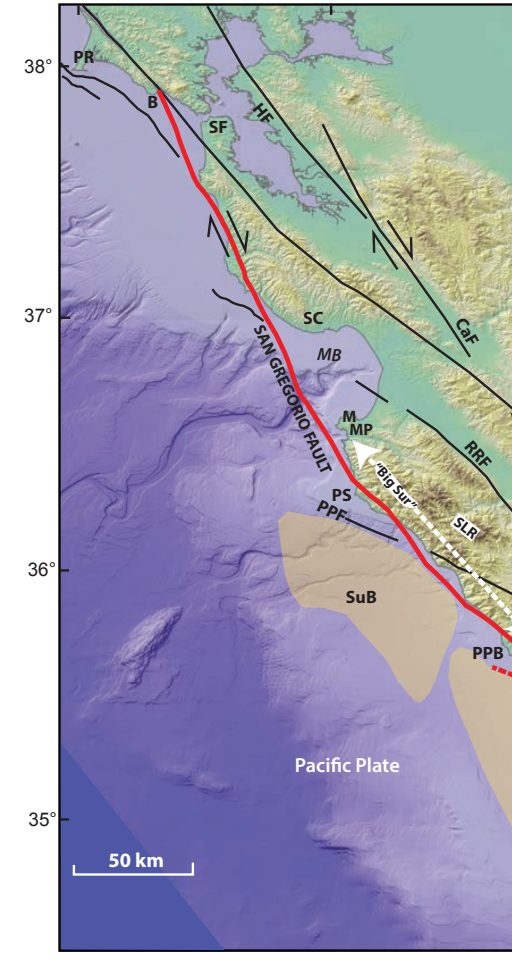

Colored shaded-relief index map of central California, showing locations of northern (San Gregorio Fault) and southern (Hosgri Fault) parts of San Gregorio–Hosgri Fault Zone (red line; dashed where uncertain). Black lines show other faults (arrows show direction of relative offset): CaF, Calaveras Fault; CF, Casmalia Fault; HF, Hayward Fault; LHF, Lions Head Fault; LOF, Los Osos Fault; NF, Nacimiento Fault; OF, Oceano Fault; PPF, Pfeiffer Point Fault; RRF, Reliz-Rinconada Fault; ShF, Shoreline Fault; SYF, Santa Ynez Fault. Gray shading shows offshore sedimentary basins (OSMB, outer Santa Maria Basin; SuB, Sur Basin); basin outlines modified from McCulloch (1987). White arrows show approximate extent of "Big Sur" region. Other abbreviations: B, Bolinas, EB, Estero Bay; M, Monterey; MB, Monterey Bay; MP, Monterey peninsula; PA, Point Arguello; PB, Point Buchon; PPB, Point Piedras Blancas; PR, Point Reyes; PS, Point Sur; SB, San Luis Obispo Bay; SC, Santa Cruz; SF, San Francisco; SLR, Santa Lucia Range.

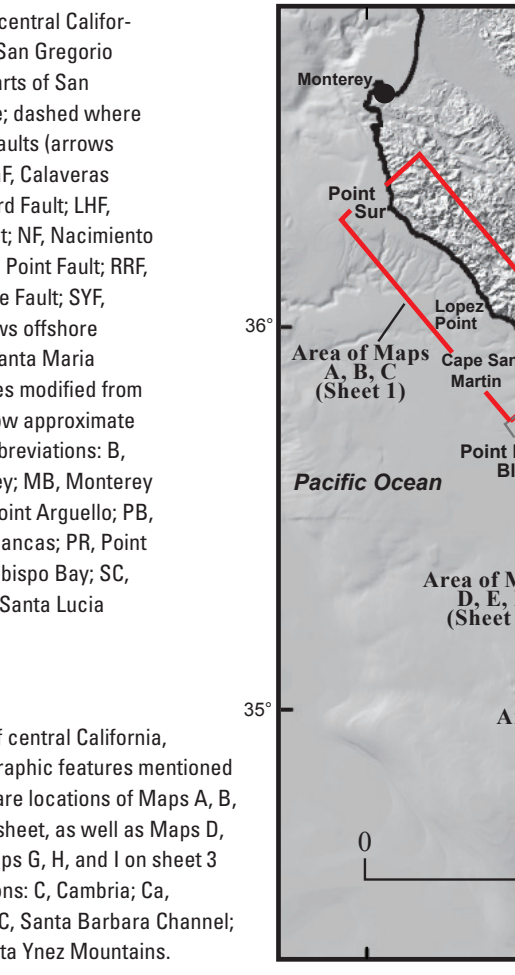

Shaded-relief index map of central California, showing locations of geographic features mentioned in this report. Also shown are locations of Maps A, B, and C (red outline) on this sheet, as well as Maps D, E, and F on sheet 2 and Maps G, H, and I on sheet 3 (gray outlines). Abbreviations: C, Cambria; Ca, Cayucos; IH, Irish Hills; SBC, Santa Barbara Channel; SS, San Simeon; SYM, Santa Ynez Mountains.

DISCUSSION

This publication consists of three map sheets that display shallow geologic structure, along with sediment distribution and thickness, for an about 225-km-long offshore section of the central California coast between Point Sur and Point Arguello. Each map sheet includes three maps, at scales of either 1:150,000 (sheets 1, 2) or 1:200,000 (sheet 3), as well as a set of either 11 or 13 figures that contain representative high-resolution seismic-reflection profiles. The maps and seismic-reflection surveys cover most of the continental shelf in this region. In addition, the maps show the locations of the shelf break and the 3-nautical-mile limit of California's State Waters.

The seismic-reflection data, which are the primary dataset used to develop the maps, were collected to support the California Seafloor Mapping Program (Johnson and others, 2017a) and U.S. Geological Survey Offshore Geologic Hazards projects. In addition to the three map sheets, this publication includes geographic information system (GIS) data files of interpreted faults, folds, sediment thicknesses, and depths-to-base of sediment. The faults and folds shown on the maps have been locally simplified as appropriate for the map scales (that is, not every fault or fold shown on the seismic-reflection profiles appears on the maps). Maps (and their databases) that show similar structure and sediment information for the adjacent Santa Barbara Channel region to the southeast are contained in Johnson and others (2017c, 2018a); Johnson and others (2015, 2016a) contain similar maps and data for the adjacent coastal area from Monterey north to Point Arena (about 325 km north of the map area).

Maps A, D, and G, on map sheets 1, 2, and 3, respectively, show tracklines for the four U.S. Geological Survey (USGS) seismic-reflection surveys that cover the Point Sur to Point Arguello region. The USGS surveys are (1) cruise B–05–11–CC, conducted in 2011 between Point Sur and Estero Bay (see Johnson and others, 2017b); (2) cruise S–6–09–SC, conducted in 2009 between Point Piedras Blancas and Point Sal (Sliter and others, 2009); (3) cruise S–6–08–SC, conducted in 2008 between Point Estero and San Luis Obispo Bay (Sliter and others, 2009); and (4) cruise 2014–632–FA, conducted in 2014 between Point Sal and Gaviota (Johnson and others, 2016b). These data were all collected using the SIG 2Mille minisparker system, which used a 500-J high-voltage electrical discharge fired 1 to 2 times per second; at normal survey speeds of 4 to 4.5 nautical miles per hour, this gives a data trace every 1 to 2 m of lateral distance covered. The single-channel data were digitally recorded in standard SEG-Y 32-bit floating-point format, using software that merges seismic-reflection data with differential GPS-navigation data. After the survey, a short-window (20 ms) automatic gain control was applied to the data, along with a 160- to 1,200-Hz bandpass filter and a heave correction that uses an automatic seafloor-detection window (averaged over 30 m of lateral distance covered). These data can resolve geologic features a few meters thick (and, hence, are considered "high-resolution"), down to subbottom depths of as much as 500 m.

A significant variation in shelf morphology is seen in this region. Shelf width steadily increases southward, from about 1 to 2 km offshore of Pfeiffer Point and the northern Big Sur region to about 8 to 9 km on the north flank of Point Piedras Blancas. Note that the "Big Sur" region does not have specific geographic boundaries, but it is generally considered to include the about 120-km-long segment of the coast between the southern Monterey peninsula and Point Piedras Blancas, as well as the adjacent about 35- to 40-km-wide Santa Lucia Range between these two northern and southern limits.

Farther south, shelf width is about 5 to 8 km between Point Piedras Blancas and Point Estero; it then increases to as much as 11 km in Estero Bay, and it decreases to about 5 km offshore of Point Buchon. South of Point Buchon, the shelf widens to as much as 18 to 21 km from San Luis Obispo Bay to Purisima Point, and it is about 10 to 13 km wide offshore of Point Arguello. Shelf gradient is as much as 2.0° to 3.0° where the shelf is narrowest in the northern Big Sur region, and it decreases to as little as about 0.3° to 0.5° as the shelf broadens in the area between San Luis Obispo Bay and Purisima Point. Where the shelf is most narrow along the Big Sur coast, it is deeply incised by submarine canyons.

Quaternary sediments and bedrock underlie the shelf. On the seismic-reflection profiles (figs. 1–36), we divide Quaternary shelf sediments into two units. The younger, upper unit (shaded blue on most seismic-reflection profiles) is generally characterized by low-amplitude, continuous to moderately continuous, diffuse, subparallel, generally flat reflections (terminology from Mitchum and others, 1977). Reflection dip ranges from relatively flat (1°–3°) on most of the shelf to moderate (as much as 11°) within and at the front of prograding sediment bars (for example, figs. 9, 10). The lower contact of this upper unit is a transgressive surface of erosion, a commonly angular, wave-cut unconformity characterized by an upward change to lower amplitude, more diffuse reflections. On the basis of this lower contact, the lower unit is inferred to have been deposited on the shelf in the last about 21,000 years during the sea-level rise that followed the last major lowstand and the Last Glacial Maximum (LGM) (Stanford and others, 2011). Global sea level was about 120 to 130 m lower during the LGM, at which time the shelf between Point Sur and Point Arguello was emergent. The post-LGM sea-level rise was rapid (about 9 to 11 m per thousand years) until about 7,000 years ago, when it slowed considerably to about 1 m per thousand years (Stanford and others, 2011).

The lower, older Quaternary (pre-LGM) unit (shaded pink where shown on the seismic-reflection profiles), which is only locally present, has three modes of occurrence: (1) In the San Luis Obispo Bay area, offshore of the mouth of the Santa Maria River (for example, figs. 27, 28, on sheet 3), it is characterized by laterally extensive, flat-lying to very gently folded, low- to moderate-amplitude, continuous, parallel reflections. (2) Between Purisima Point and Point Piedras Blancas, the strata are present in thin lenses and as low-relief channel fills (for example, figs. 16, 17, 21, 29, on sheets 2, 3) that have internal diffuse, low-amplitude reflections. (3) Between Point Buchon and Point Piedras Blancas, the unit is present as the shallow, commonly warped fill of fault-bounded basins within and adjacent to the Hosgri Fault Zone (for example, figs. 19, 20, 21, 24, on sheet 2). Although variable in their occurrence, these older Quaternary shelf units are all inferred to have been deposited in shelf and marginal-marine environments during repeated Quaternary sea-level fluctuations (Miller and others, 2005).

Quaternary deposits (shaded green on many seismic-reflection profiles) are also present seaward of the shelf and shelf break on the upper slope. North of Cape San Martin, these slope-to-proximal basin deposits mainly form sedimentary wedges that are in fault contact with uplifted bedrock (for example, figs. 2, 3, 4, 5, 6, 7, 8). Strata within these wedges are represented by a mix of parallel, lenticular, and hummocky, offshore-dipping reflections, consistent with deposition by processes ranging from dilute sediment gravity flows to submarine landslides. Slope deposits south of Cape San Martin (see, for example, figs. 9, 10, 13; see also, figs. 15, 17, 18, 19, 20, 21, 22, 23, 24, 25, on sheet 2) are characterized by moderate-amplitude, moderately continuous, subparallel, offshore-dipping reflections. These slope deposits contain numerous internal erosional surfaces and disconformities, inferred to have formed as the shelf prograded seaward during Quaternary sea-level regressions and lowstands.

Seafloor bedrock outcrops form rough, irregular, hummocky seafloor outcrops on high-resolution bathymetric imagery (Maps A, D, and G, on sheets 1, 2, and 3; National Oceanic and Atmospheric Administration, 2018). Bedrock outcrops are most abundant on the inner shelf, but they locally extend to the midshelf and outer shelf areas between Lopez Point (this sheet) and Point Buchon (sheet 2). Older Mesozoic basement units include rocks of the Jurassic and Cretaceous Franciscan Complex and the Jurassic Coast Range Ophiolite (see, for example, Watt and others, 2015), correlative with adjacent coastal outcrops mapped by Woodring and Bramlette (1950) at Point Sal, by Hall (1974, 1976) and Hall and others (1979) between Point Buchon and Point Piedras Blancas, and by Graymer and others (2014) and Rosenberg and Wills (2016) between Point Piedras Blancas and Point Sur. Diverse lithologies include mélange, sandstone, chert, mafic volcanic rocks, and serpentinite. These deformed Mesozoic basement rocks are typically massive or "reflection free," and they cannot be subdivided on our seismic-reflection profiles; there, they are labeled "Ku" ("Late Cretaceous sandstone and interbedded claystone"; Watt and others, 2015) or "KJu" ("undivided Jurassic and Cretaceous bedrock").

Neogene sedimentary rocks are present beneath the shelf in the subsurface south of Cape San Martin. On high-resolution seismic-reflection profiles (for example, figs. 11–13), these strata commonly yield parallel to subparallel, continuous, variable-amplitude, high-frequency reflections. These Neogene strata are cut by numerous faults and commonly are folded, having dips too steep to be imaged in many places on seismic-reflection profiles. Local zones that lack reflections probably also result from the presence of interstitial gas within the sediments (for example, fig. 34, on sheet 3), largely derived from the Miocene Monterey Formation, the primary petroleum source rock in the adjacent offshore Santa Maria Basin and Sur Basin (McCulloch, 1987; Mayerson, 1997). This effect has been referred to as "gas blanking," "acoustic turbidity," or "acoustic masking" (Hovland and Judd, 1988; Fader, 1997). The gas scatters or attenuates the acoustic energy, preventing penetration.

In addition to the Monterey Formation, Neogene strata that crop out along the coast and are present at least beneath the inner shelf include Miocene diabase and basalt, the Miocene Obispo Formation, the Miocene Lospe Formation, the Miocene Point Sal Formation, the Miocene Tranquillon Volcanics, the Miocene and Pliocene Pismo Formation, the Miocene and Pliocene Sisquoc Formation, and the Pliocene Foxen Mudstone (Hoskins and Griffiths, 1971; McCulloch, 1987; Willingham and others, 2013; Watt and others, 2015). Because our focus is on Quaternary sediments and structure, we have not attempted to delineate these units on our shallow seismic-reflection profiles, where we have grouped them as "Nu" ("undivided Neogene strata").

Faults shown on the seismic-reflection profiles (figs. 1–36) are identified on the basis of the abrupt truncation or warping of reflections and (or) the juxtaposition of reflection panels that have differing seismic parameters, such as reflection presence, amplitude, frequency, geometry, continuity, and vertical sequence. The right-lateral San Gregorio–Hosgri Fault (see Maps A, D, and G, on sheets 1–3; see also, figs. 2–13, and colored shaded-relief index map, on this sheet; figs. 16–25, on sheet 2; and figs. 26, 27, 29, 31–34, on sheet 3) is the most significant structure in the map area. On a regional scale, the San Gregorio–Hosgri Fault (SGHF) is part of a 400-km-long, right-lateral fault system that extends northwestward from Point Arguello to the area offshore of San Francisco, where it merges with the San Andreas Fault (Dickinson and others, 2005: Langenheim and others, 2013; Colgan and Stanley, 2016). From north to south in this part of central California, the SGHF lies offshore between the south flank of Point Sur and the north flank of Point Piedras Blancas, then comes onshore at Point Piedras Blancas before heading offshore again between the south flank of Point Piedras Blancas and Point Arguello. On the seismic-reflection profiles, we label this structure the Hosgri Fault south of Point Piedras Blancas and, north of Point Piedras Blancas and south of Point Sur, the San Gregorio–Hosgri Fault system. The part of this long, continuous fault zone that is near Point Piedras Blancas has also been referred to as the San Simeon Fault (see, for example, Lettis and others, 2004).

Cumulative fault offset along the SGHF is as much as 150 to 160 km, decreasing to the south by transferring slip on to northwest-striking faults that converge with the SGHF both onland and offshore from the east (Langenheim and others, 2013; Colgan and Stanley, 2016). In the map area, the offshore-converging faults include the Los Osos Fault (fig. 22, on sheet 2) and the Shoreline–Point Buchon Fault (fig. 24, on sheet 2), on the northeast and southwest flanks of Point Buchon; and the Casmalia Fault (figs. 28, 30, on sheet 3) and the Lions Head Fault (figs. 30, 31, on sheet 3) on the northeast and southwest flanks of Point Sal.

Johnson and Watt (2012) and Johnson and others (2018b) provided detailed documentation of the SGHF in the part of the map area that lies north of Point Sal; the documentation is based on seismic-reflection profiles, marine magnetic data, and new high-resolution bathymetry. Between Point Sur and Point Piedras Blancas (see Map A), the SGHF is a continuous zone characterized by multiple strands, stepovers, bathymetric scarps and lineaments, shutter ridges, deflected drainages, and other geomorphic features that are consistent with active strike-slip faulting. The SGHF forms the eastern margin of the Sur Basin (McCulloch, 1987). A more northwest-striking structure, the Pfeiffer Point Fault (fig. 1) diverges from the SGHF to form the northeastern margin of the Sur Basin and also the southwest flank of Point Sur.

Between Point Piedras Blancas and Point Arguello, the Hosgri Fault forms a zone characterized by small bends, multiple splays, and local uplifts and basins (Johnson and Watt, 2012). The fault zone divides into east and west splays offshore of Point Estero (see Map D, on sheet 2). The east splay extends onshore on the south flank of Point Piedras Blancas, then it heads back into the offshore at Ragged Point on the north flank of Point Piedras Blancas (Graymer and others, 2014). The west splay bends to the northwest, becoming a blind oblique-thrust fault overlain by a fold belt in the offshore, on the southwest flank of Point Piedras Blancas (see, for example, fig. 16, on sheet 2; see also, Johnson and Watt, 2012). The Hosgri Fault and the fold belt offshore of Point Piedras Blancas form the eastern and northeastern boundaries of the offshore Santa Maria Basin (McCulloch, 1987).

At its south end (figs. 33, 34, on sheet 3) between Point Arguello and Purisima Point, the Hosgri Fault Zone is thought to terminate in east-west-striking reverse-slip faults (for example, the Santa Ynez River Fault) and folds that extend into the offshore from the western part of the Santa Ynez Mountains (Steritz and Luyendyk, 1994; Sorlien and others, 1999). The Point Arguello area thus occupies a significant transitional tectonic zone between the north-northwest-striking, strike-slip Hosgri Fault and the east-west-striking contractional structures and high structural and topographic relief of the Santa Ynez Mountains and Santa Barbara Channel (Johnson and others, 2018a).

On sheets 1, 2, and 3, Maps B, E, and H show the thickness of the post-LGM depositional unit (blue shading on most seismic-reflection profiles), and Maps C, F, and I show the depth to the base of this unit. To make these maps, water bottom and depth to base of the uppermost Pleistocene and Holocene sediment layer were mapped from seismic-reflection profiles. The difference between the two horizons was exported for every shot point as XY coordinates (UTM zone 10) and two-way travel time (TWT). The thickness of the uppermost Pleistocene and Holocene unit (Maps B, E, and H) was determined by applying an estimated sound velocity of 1,600 m/sec to the TWT. The thickness points were interpolated to a preliminary continuous surface, overlaid with zero-thickness bedrock outcrops, and contoured, following the methodology of Wong and others (2012). The data points from seismic-reflection profiles are dense along tracklines (about 1–2 m apart) and sparse between tracklines (typically 800–1,000 m apart), resulting in contouring artifacts. Contours were therefore manually edited in a few areas to incorporate the effect of faults, to remove irregularities from interpolation, and to reflect other geologic information and complexity. Contour modifications and regridding were repeated a few times to produce the final maps. Data for the depth to base of the uppermost Pleistocene and Holocene unit (Maps C, F, and I) were generated by adding the thickness data to water depths determined from bathymetric mapping (Maps A, D, and G). The area covered in Maps B, E, and H and Maps C, F, and I extends from the eastern extent of the seismic tracklines (typically the inner shelf, at water depths of 10 to 15 m) to either the western extent of trackline coverage (generally the outer shelf) or to the shelf break.

Within this about 225-km-long region of open coast, 11 different "domains" of shelf sediment are delineated on the basis of coastal geomorphology and sediment thickness (Maps B, E, and H, on sheets 1, 2, 3). Coastal relief and sediment supply are variable across this region; however, all domains are exposed to the wave-dominated, open Pacific coast, the highest wave energy being focused at coastal promontories (for example, Point Buchon, Point Sal, Purisima Point, Point Arguello). Table 1 summarizes the size, mean sediment thickness, and sediment volume of each domain.

(1) The Point Sur shelf domain (Map B) lies on the narrow (about 2–5 km) shelf on the southwest flank of Point Sur. The mouth of the Big Sur River (watershed, about 160 km²), which is located at the north end of the domain, is the inferred largest sediment source. South of the Big Sur River mouth, the coast is characterized by much smaller (<10 km²) watersheds and steep coastal cliffs. Maximum sediment thickness (about 21 m) is found in an onshore- and offshore-thinning lens (fig. 1) centered at midshelf depths (about 40 m). Mean sediment thickness in the Point Sur shelf domain is 6.8 m. The domain is bounded to the southeast by informally named Partington submarine canyon, which intersects southward littoral-sediment drift and is a conduit for offshore sediment transport to the Sur Basin.

(2) The north Big Sur shelf domain (Map B) is characterized by a very narrow (≤2 km) shelf that lies between the San Gregorio–Hosgri Fault and the steep (as much as 10°), rapidly uplifting (Ducea and others, 2003) Big Sur coast. Sediment is provided by relatively small (generally less than 10 km²) watersheds that extend 2 to 10 km inland into the Santa Lucia Range. Mean sediment thickness is 9.3 m, and maximum sediment thickness (about 26 m) is found in prograding bars that extend from the inner shelf, at water depths of about 22 m, to the shelf break (figs. 2, 3, 4). This domain is incised by several tributary heads of the informally named Lucia submarine canyon.

(3) The central Big Sur shelf domain (Map B) is characterized by a wider (3–5 km) shelf on the north and south flanks of Lopez Point, which also is offshore of the steep, rapidly uplifting Santa Lucia Range coast and is bounded on the west by the San Gregorio–Hosgri Fault. Mean sediment thickness is 9.9 m. The thickest sediment (about 38 m) is found in a prograding bar offshore of the mouth of Limekiln Creek, at water depths of about 40 m.

(4) The south Big Sur shelf domain (Map B; see also, Map E, on sheet 2) extends from the south flank of Lopez Point to the north flank of Point Piedras Blancas, an area where the shelf progressively widens from about 4 to 8 km. As with the north and central Big Sur domains to the north, the thickest sediment (about 28 m) is found in prograding bars near the mouths of a network of small, steep coastal watersheds. Mean sediment thickness is 9.7 m. The shelf in this domain is crossed obliquely by the San Gregorio–Hosgri Fault, which has only a minor influence (for example, fig. 10) on sediment thickness.

(5) The Cambria shelf domain (Map E, on sheet 2) extends from the north flank of Point Piedras Blancas to the northern part of Estero Bay. Bedrock crops out on much of the inner shelf, and it locally extends to the midshelf and outer shelf areas. Mean sediment thickness is 3.0 m. Maximum sediment thickness (about 18 m) is found as the upper fill of fault-bounded basins within and adjacent to the Hosgri Fault Zone. Direct sediment supply is from coastal watersheds such as Santa Rosa Creek (190 km²), which are larger and extend farther (15–20 km) inland than drainages along the much steeper Big Sur coast to the north.

(6) The relatively small Estero Bay domain (Map E, on sheet 2) is located in the central part of Estero Bay, offshore of Morro Bay (both the estuary and the city). Offshore sediment is found in two troughs that represent lowstand paleochannels associated with the Cayucos Creek composite watershed (223 km²) to the north (fig. 21, on sheet 2) and the Morro Bay composite watershed (190 km²) to the south (fig. 22, on sheet 2). The locations of paleochannels are, at least in part, structurally controlled; the Morro Bay paleochannel aligns with uplifts on the north flank of the Los Osos Fault Zone. Maximum sediment thickness (about 21 m) is found in a small basin within the Cayucos Creek paleochannel in the zone of convergence between the Los Osos and Hosgri Faults. Mean sediment thickness in the Estero Bay domain is 5.4 m.

(7) The Point Buchon shelf domain (Maps E, H, on sheets 2, 3) extends from the southern part of Estero Bay to the south flank of Point Buchon. Significant bedrock outcrops are present in the inner shelf to midshelf areas, and the thickest sediment (about 11 m) is found in outer shelf basins within the Hosgri Fault Zone (fig. 24, on sheet 2). Mean sediment thickness is 2.2 m. Adjacent sediment sources are small coastal watersheds whose headwaters are in the Irish Hills (for example, Islay Creek).

(8) The Santa Maria River delta domain (Map H, on sheet 3) lies within a structural trough between the Shoreline-Oceano Fault Zone and Point Buchon to the north and the Casmalia Fault and Point Sal to the south. The domain lies offshore of the mouth of the Santa Maria River watershed, one of the largest (4,558 km², including large tributaries) coastal watersheds in California. The river feeds a large, shore-parallel midshelf (water depths, about 40–70 m) depocenter (figs. 27, 28, 29, on sheet 3) that has a maximum sediment thickness of 31 m. Mean sediment thickness in the domain is 17.2 m.

(9) The Point Sal to Purisima Point domain (Map H, on sheet 3) is bounded on the north and south by saddlelike zones of diminished shelf-sediment thicknesses offshore of Point Sal and Purisima Point. The domain is characterized by an inner shelf to midshelf, shore-parallel depocenter (figs. 31, 32, on sheet 3) that has a maximum sediment thickness of 43 m. Mean sediment thickness on the shelf in this domain is 18.0 m, and sediment thickness notably decreases west of the depocenter; however, our surveys and the sediment maps do not extend to the shelf break for this entire area. The depocenter in this domain is notably not paired with a large onland alluvial-sediment source; San Antonio Creek is the largest (about 400 km²) adjacent coastal watershed, which is much smaller than both the Santa Maria River watershed (4,558 km²) to the north and the Santa Ynez River watershed (2,323 km²) to the south. The presence of thick sediment in this depocenter may, thus, indicate significant lateral shelf-sediment transport from domains to the north and (or) south.

(10) The Santa Ynez River delta domain (Map H, on sheet 3), which extends southward from Purisima Point to the south flank of Point Arguello, is similarly characterized by an inner shelf to midshelf, shore-parallel depocenter (figs. 33, 34, 35, on sheet 3). Maximum sediment thickness in the depocenter is 44 m. Mean sediment thickness in the domain is 25.6 m; however, our surveys and maps do not extend to the shelf break, and so the mean thickness across the entire shelf is almost certainly less. The domain lies offshore of the mouth of the large (2,323 km²) Santa Ynez River watershed, clearly the dominant sediment source.

(11) The northern part of the Point Arguello to Point Conception domain (Map H, on sheet 3) lies within our map area; the structure and sediment distribution in the southern part of this domain are shown in Johnson and others (2018a). Within our map area, mean and maximum sediment thicknesses are 6.2 m and 18 m, respectively. Small coastal watersheds that drain the western Santa Ynez Mountains are the inferred primary sediment source. It is also possible that the shelf in our map area receives sediment derived from the Santa Ynez River; however, this would require about 25 km of southward sediment transport around Point Arguello.

Mean sediment thickness for the entire shelf in our map area between Point Sur and Point Arguello is 12.2 m, and total sediment volume is $24{,}728\times10^6$ m^3, similar to the mean sediment thickness (14.1 m) for the about 120-km-long, mainland (northern) part of the Santa Barbara Channel shelf to the southeast (Johnson and others, 2017c). Sediment distribution and thickness varies substantially in both regions, largely in response to variations in sediment supply and both local and regional tectonics.

Table 1. Area, sediment-thickness, and sediment-volume data for the 11 regional shelf-sediment domains mapped between Point Sur and Point Arguello, in central California.

Domain	Area (km^2)	Mean sediment thickness (m)	Sediment volume (10^6 m^3)
(1) Point Sur shelf	37.7	6.8	257
(2) North Big Sur shelf	18.3	9.3	170
(3) Central Big Sur shelf	40.0	9.9	396
(4) South Big Sur shelf	156.4	9.7	1,524
(5) Cambria shelf	337.5	3.0	1,000
(6) Estero Bay	102.8	5.4	559
(7) Point Buchon shelf	253.3	2.2	564
(8) Santa Maria River delta	372.7	17.2	6,407
(9) Point Sal to Purisima Point	307.2	18.0	5,543
(10) Santa Ynez River delta	301.3	25.6	7,703
(11) Point Arguello to Point Conception (northern part within this map area)	97.4	6.2	605
Entire Point Sur to Point Arguello region	2,024.5	12.2	24,728

REFERENCES CITED

Colgan, J.P., and Stanley, R.G., 2016, The Point Sal–Point Piedras Blancas correlation and the problem of slip on the San Gregorio–Hosgri fault, central California Coast Ranges: Geosphere, v. 12, p. 971–984.

Dickinson, W.R., Ducea, M., Rosenberg, L.I., Greene, H.G., Graham, S.A., Clark, J.C., Weber, G.E., Kidder, S., Ernst, W.G., and Brabb, E.E., 2005, Net dextral slip, Neogene San Gregorio-Hosgri Fault Zone, coastal California—Geologic evidence and tectonic implications: Geological Society of America Special Paper 391, 43 p.

Ducea, M, House, M.A., and Kidder, S., 2003, Late Cenozoic denudation and uplift rates in the Santa Lucia Mountains, California: Geology, v. 31, p. 139–142.

Fader, G.B.J., 1997, Effects of shallow gas on seismic-reflection profiles, *in* Davies, T.A., Bell, T., Cooper, A.K., Josenhaus, H., Polyak, L., Solheim, A., Stoker, M.S., and Stravers, J.A., eds., Glaciated continental margins—An atlas of acoustic images: London, Chapman & Hall, p. 29–30.

Graymer, R.W., Langenheim, V.E., Roberts, M.A., and McDougall, Kristin, 2014, Geologic and geophysical maps of the eastern three-fourths of the Cambria 30′×60′ quadrangle, central California Coast Ranges: U.S. Geological Survey Scientific Investigations Map 3287, map sheets 1:100,000 scale (interactive PDF), pamphlet 50 p., https://doi.org/10.3133/sim3287.

Hall, C.A., 1974, Geologic map of the Cambria region, San Luis Obispo County, California: U.S. Geological Survey Miscellaneous Field Studies Map MF–599, 2 sheets, scale 1:24,000.

Hall, C.A., 1976, Geologic map of the San Simeon–Piedras Blancas region, San Luis Obispo County, California: U.S. Geological Survey Miscellaneous Field Studies Map MF–784, scale 1:24,000.

Hall, C.A., Jr., Ernst, W.G., Prior, S.W., and Wiese, J.W., 1979, Geologic map of the San Luis Obispo–San Simeon region, California: U.S. Geological Survey Miscellaneous Investigations Series Map I–1097, 3 sheets, scale 1:48,000.

Hoskins, E.G., and Griffiths, J.R., 1971, Hydrocarbon potential of northern and central California offshore, *in* Cram, I.H., ed., Future petroleum provinces of the United States—Their geology and potential: American Association of Petroleum Geologists Memoir 15, v. 1, p. 212–228.

Hovland, M., and Judd, A.G., 1988, Seabed pockmark and seepages: London, Graham & Trotman, Inc., 293 p.

Johnson, S.Y., Cochrane, G.R., Golden, N.E., Dartnell, P., Hartwell, S.R., Cochran, S.A., and Watt, J.T., 2017a, The California Seafloor and Coastal Mapping Program—Providing science and geospatial data for California's State Waters: Ocean and Coastal Management, v. 140, p. 88–104.

Johnson, S.Y., Dartnell, P., Cochrane, G.R., Hartwell, S.R., Golden, N.E., Kvitek, R.G., and Davenport, C.W. (S.Y. Johnson and S.A. Cochran, eds.), 2018a, California State Waters Map Series—Offshore of Point Conception, California: U.S. Geological Survey Open-File Report 2018–1024, pamphlet 36 p., 9 sheets, scale 1:24,000, https://doi.org/10.3133/ofr20181024.

Johnson, S.Y., Dartnell, P., Golden, N.E., Hartwell, S.R., Erdey, M.D., Greene, H.G., Cochrane, G.R., Kvitek, R.G., Manson, M.W., Endris, C.A., Dieter, B.E., Watt, J.T., Krigsman, L.M., Sliter, R.W., Lowe, E.N., and Chin, J.L. (S.Y. Johnson and S.A. Cochran, eds.), 2015, California State Waters Map Series—Offshore of Salt Point, California: U.S. Geological Survey Open-File Report 2015–1098, pamphlet 37 p., 10 sheets, scale 1:24,000, https://doi.org/10.3133/ofr20151098.

Johnson, S.Y., Dartnell, P., Hartwell, S.R., Cochrane, G.R., Golden, N.E., Watt, J.T., Davenport, C.W., Kvitek, R.G., Erdey, M.D., Krigsman, L.M., Sliter, R.W., and Maier, K.L. (S.Y. Johnson and S.A. Cochran, eds.), 2016a, California State Waters Map Series—Offshore of Monterey, California: U.S. Geological Survey Open-File Report 2016–1110, pamphlet 44 p., 10 sheets, scale 1:24,000, https://doi.org/10.3133/ofr20161110.

Johnson, S.Y., Hartwell, S.R., and Beeson, J.W., 2016b, Marine geophysical data—Point Sal to Refugio State Beach, southern California: U.S. Geological Survey data release, https://doi.org/10.5066/F7SX6BCD.

Johnson, S.Y., Hartwell, S.R., Sliter, R.W., and Beeson, J.W., 2017b, Minisparker seismic-reflection data of field activity B–05–11–CC, from Point Sur to Morro Bay, offshore central California, 2011–09–12 to 2011–09–26: U.S. Geological Survey, National Archive of Marine Seismic Surveys database, available at https://walrus.wr.usgs.gov/namss/survey/b-05-11-cc/.

Johnson, S.Y., Hartwell, S.R., Sorlien, C.C., Dartnell, P., and Ritchie, A.R., 2017c, Shelf evolution along a transpressive transform margin, Santa Barbara Channel, California: Geosphere, v. 13, no. 6, p. 2041–2077.

Johnson, S.Y., and Watt, J.T., 2012, Influence of fault trend, bends, and convergence on shallow structure and geomorphology of the Hosgri strike-slip fault, offshore Central California: Geosphere, v. 8, no. 6, p. 1632–1656.

Johnson, S.Y., Watt, J.T., Hartwell, S.R., and Kluesner, J.W., 2018b, Neotectonics of the Big Sur Bend, San Gregorio-Hosgri fault system, central California: Tectonics, v. 37, p. 1930–1954, https://doi.org/10.1029/2017TC004724.

Langenheim, V.E., Jachens, R.C., Graymer, R.W., Colgan, J.P., Wentworth, C.M., and Stanley, R.G., 2013, Fault geometry and cumulative offsets in the central Coast Ranges, California—Evidence for northward increasing slip along the San Gregorio–San Simeon–Hosgri fault: Lithosphere, v. 5, no. 1, p. 29–48.

Lettis, W.R., Hanson, K.L., Unruh, J.R., McLaren, M., and Savage, W.U., 2004, Quaternary tectonic setting of south-central coastal California, chap. AA *of* Keller, M.A., ed., Evolution of sedimentary basins/offshore oil and gas investigations—Santa Maria Province: U.S. Geological Survey Bulletin 1995–AA, 21 p., 1 plate, scale 1:250,000, available at https://pubs.usgs.gov/bul/1995/aa/.

Mayerson, D., 1997, Santa Maria-Partington basin, *in* Dunkel, C.A., and Piper, K.A., eds., 1995 National assessment of oil and gas resources of the Pacific Outer Continental Shelf Region: U.S. Department of the Interior, Minerals Management Service, OCS Report MMS 97–0019, p. 84–95.

McCulloch, D.S., 1987, Regional geology and hydrocarbon potential of offshore central California, *in* Scholl, D.W., Grantz, A., and Vedder, J.G., eds., Geology and resource potential of the continental margin of western North America and adjacent ocean basins—Beaufort Sea to Baja California: Circum-Pacific Council for Energy and Mineral Resources, Earth Science Series, v. 6., p. 353–401.

Miller, K.G., Kominz, M.A., Browning, J.V., Wright, J.D., Mountain, G.S., Katz, M.E., Sugarman, P.J., Cramer, B.S., Christie-Blick, N., and Pekar, S.F., 2005, The Phanerozoic record of global sea-level change: Science, v. 310, p. 1293–1298.

Mitchum, R.M., Jr., Vail, P.R., and Sangree, J.B., 1977, Seismic stratigraphy and global changes of sea level, part 6—Stratigraphic interpretation of seismic reflection patterns in depositional sequences, *in* Payton, C.E., ed., Seismic stratigraphy—Applications to hydrocarbon exploration: Tulsa, Okla., American Association of Petroleum Geologists, p. 117–133.

National Centers for Environmental Information, 2012, U.S. Coastal Relief Model—Southern California version 2: National Oceanic and Atmospheric Administration, National Centers for Environmental Information database, accessed October 20, 2017, at https://www.ngdc.noaa.gov/mgg/coastal/crm.html.

National Oceanic and Atmospheric Administration, 2018, Digital Coast: National Oceanic and Atmospheric Administration Office for Coastal Management website, accessed March 2018, at https://coast.noaa.gov/digitalcoast/.

Rosenberg, L.I., and Wills, C.J., compilers, 2016, Preliminary geologic map of the Point Sur 30′×60′ quadrangle, California, version 1.0: California Geological Survey, scale 1:100,000, available at ftp://ftp.consrv.ca.gov/pub/dmg/rgmp/Prelim_geo_pdf/.

Sliter, R.W., Triezenberg, P.J., Hart, P.E., Watt, J.T., Johnson, S.Y., and Scheirer, D.S., 2009, High-resolution seismic-reflection and marine magnetic data along the Hosgri Fault Zone, central California: U.S. Geological Survey Open-File Report 2009–1100, available at https://pubs.usgs.gov/of/2009/1100/.

Sorlien, C.C., Kamerling, M.J., and Mayerson, D., 1999, Block rotation and termination of the Hosgri strike-slip fault, California, from three-dimensional map restoration: Geology, v. 27, no. 11, p. 1039–1042.

Stanford, J.D., Hemingway, R., Rohling, E.J., Challenor, P.G., Medina-Elizalde, M., and Lester, A.J., 2011, Sea-level probability for the last deglaciation—A statistical analysis of far-field records: Global and Planetary Change, v. 79, nos. 3–4, p. 193–203, https://doi.org/10.1016/j.gloplacha.2010.11.002.

Steritz, J.W., and Luyendyk, B.P., 1994, Hosgri fault zone, offshore Santa Maria Basin, California, *in* Alterman, I.B., McMullen, R.B., Cluff, L.S., and Slemmons, D.B., eds., Seismotectonics of the central California Coast Ranges: Geological Society of America Special Paper 292, p. 191–209.

Watt, J.T., Johnson, S.Y., Hartwell, S.R., and Roberts, M., 2015, Offshore geology and geomorphology from Point Piedras Blancas to Pismo Beach, San Luis Obispo County, California: U.S. Geological Survey Scientific Investigations Map 3327, pamphlet 6 p., 6 sheets, scale 1:35,000, https://doi.org/10.3133/sim3327.

Willingham, C.R., Rietman, J.D., Heck, R.G., and Lettis, W.R., 2013, Characterization of the Hosgri Fault Zone and adjacent structures in the offshore Santa Maria Basin, south-central California, chap. CC *of* Keller, M.A., ed., Evolution of sedimentary basins/offshore oil and gas investigations—Santa Maria Province: U.S. Geological Survey Bulletin 1995–CC, 105 p., 7 plates, scale 1:200,000, available at https://pubs.usgs.gov/bul/1995/cc/.

Woodring, W.P., and Bramlette, M.N., 1950, Geology and paleontology of the Santa Maria district, California: U.S. Geological Survey Professional Paper 222, 185 p., 6 plates, scale 1:24,000.

Wong, F.L., Phillips, E.L., Johnson, S.Y, and Sliter, R.W., 2012, Modeling of depth to base of Last Glacial Maximum and seafloor sediment thickness for the California State Waters Map Series, eastern Santa Barbara Channel, California: U.S. Geological Survey Open-File Report 2012–1161, 16 p., available at https://pubs.usgs.gov/of/2012/1161/.

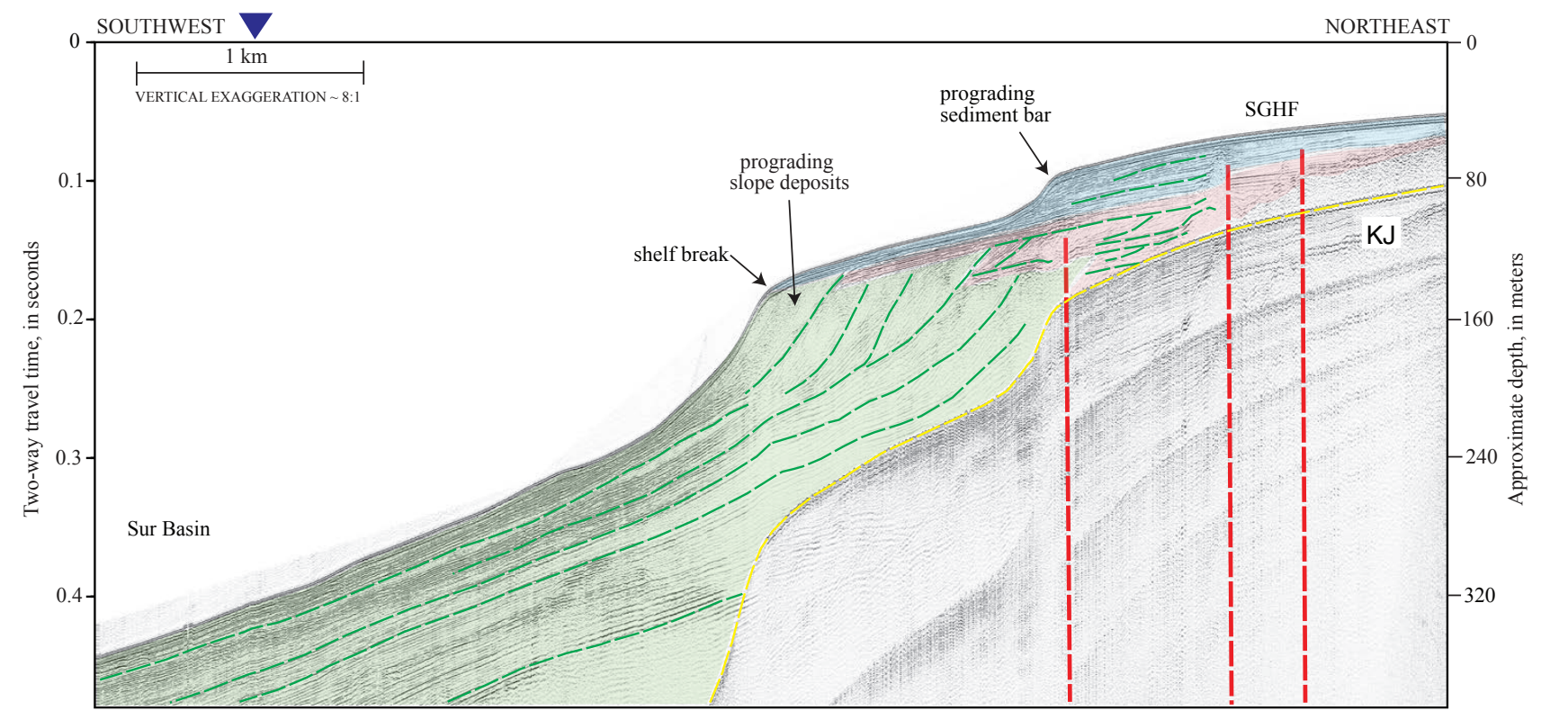

Figure 10. USGS high-resolution minisparker seismic-reflection profile BSS–87 (collected in 2011 on survey B–05–11–CC), which crosses shelf south-southwest of Cape San Martin; see Map A for location. Dashed red lines show faults, including strands of San Gregorio–Hosgri Fault Zone (SGHF). Blue shading shows inferred uppermost Pleistocene and Holocene strata, deposited since last sea-level lowstand (Last Glacial Maximum, LGM), about 21,000 years ago. Pink shading shows pre-LGM Quaternary sediment. Green shading shows Quaternary slope deposits. 'KJ,' rocks of the Jurassic and Cretaceous Franciscan Complex. Dashed green lines highlight continuous reflections (not intended to show correlations across faults). Dashed yellow line is seafloor multiple (echo of seafloor reflector). Purple triangle shows approximate location of California's State Waters limit (yellow line on Maps A, B, C).

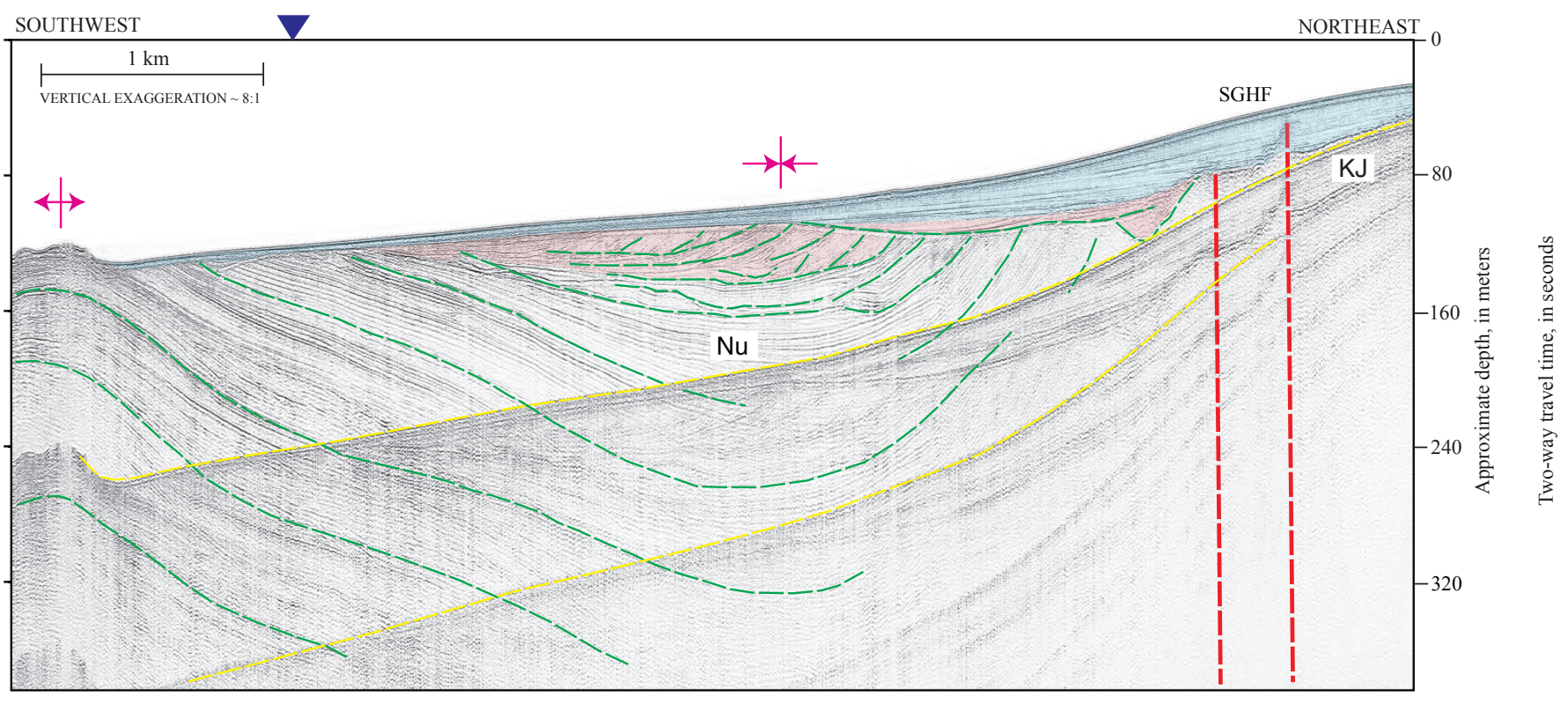

Figure 11. USGS high-resolution minisparker seismic-reflection profile BSS–81 (collected in 2011 on survey B–05–11–CC), which crosses shelf south of Cape San Martin; see Map A for location. Dashed red lines show strands of San Gregorio–Hosgri Fault Zone (SGHF). Magenta symbols show fold axes (diverging arrows, anticline; converging arrows, syncline). Blue shading shows inferred uppermost Pleistocene and Holocene strata, deposited since last sea-level lowstand (Last Glacial Maximum, LGM), about 21,000 years ago. Pink shading shows pre-LGM Quaternary sediment. 'Nu,' undivided Neogene strata; 'KJ,' rocks of the Jurassic and Cretaceous Franciscan Complex. Dashed green lines highlight continuous reflections (not intended to show correlations across faults). Dashed yellow lines are seafloor multiples (echoes of seafloor reflector). Purple triangle shows approximate location of California's State Waters limit (yellow line on Maps A, B, C).

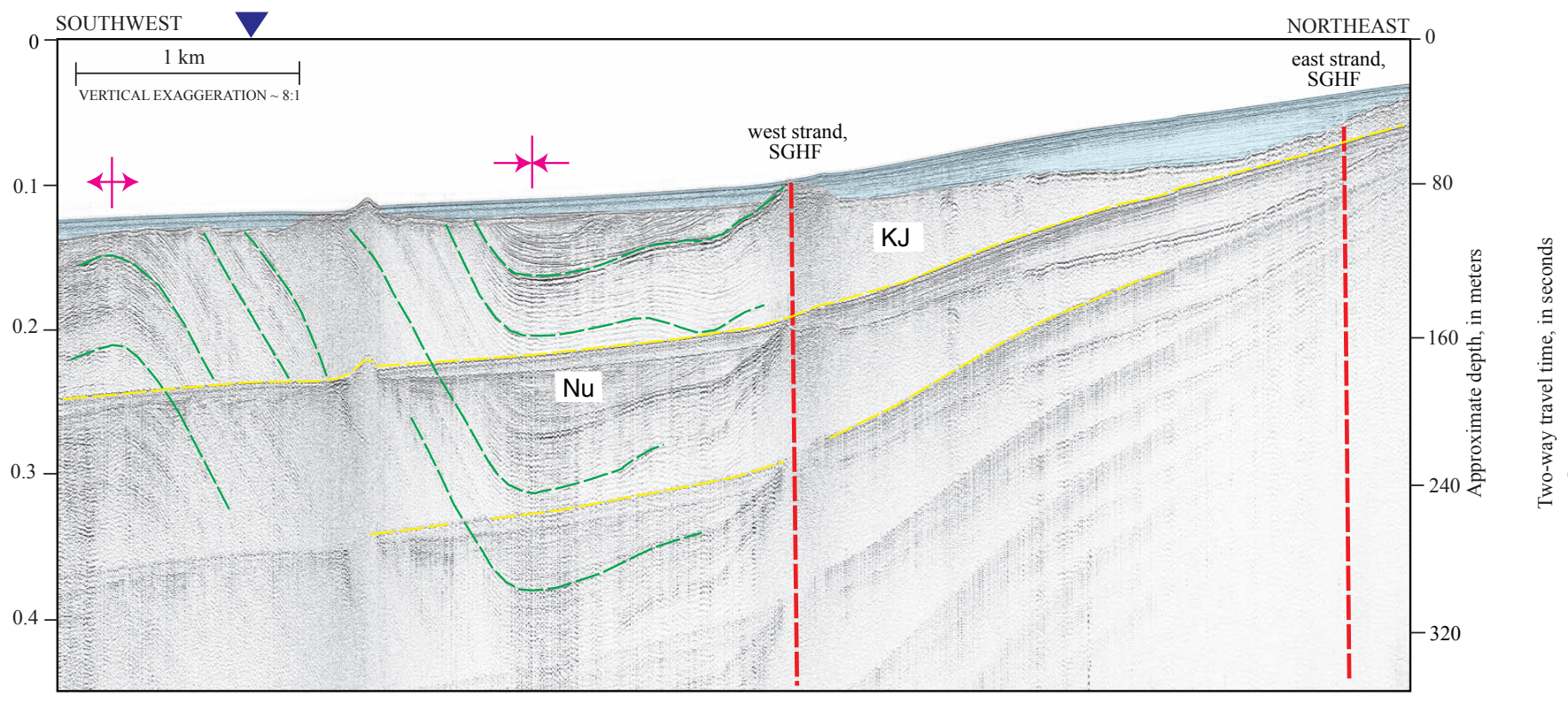

Figure 12. USGS high-resolution minisparker seismic-reflection profile BSS–74A (collected in 2011 on survey B–05–11–CC), which crosses shelf about midway between Cape San Martin and Ragged Point; see Map A for location. Dashed red lines show west and east strands of San Gregorio–Hosgri Fault Zone (SGHF). Magenta symbols show fold axes (diverging arrows, anticline; converging arrows, syncline). Blue shading shows inferred uppermost Pleistocene and Holocene strata, deposited since last sea-level lowstand about 21,000 years ago. 'Nu,' undivided Neogene strata; 'KJ,' rocks of the Jurassic and Cretaceous Franciscan Complex. Dashed green lines highlight continuous reflections (not intended to show correlations across faults). Dashed yellow lines are seafloor multiples (echoes of seafloor reflector). Purple triangle shows approximate location of California's State Waters limit (yellow line on Maps A, B, C).

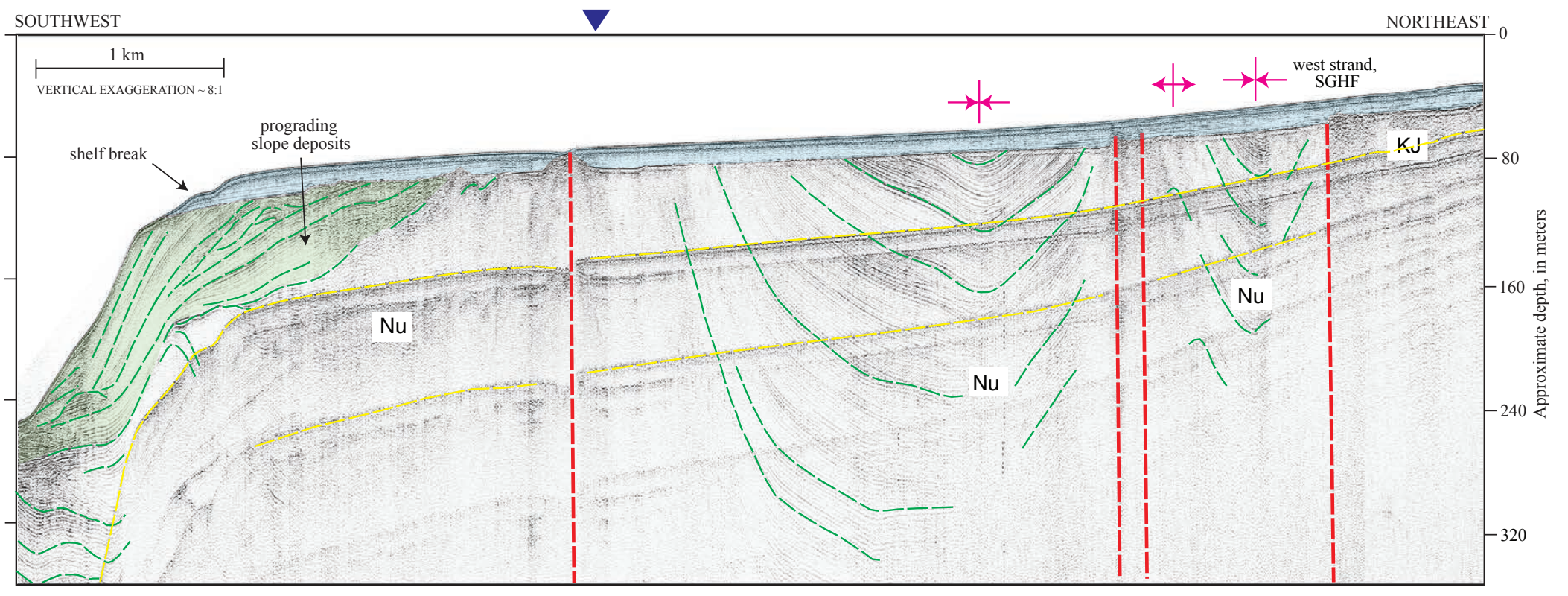

Figure 13. USGS high-resolution minisparker seismic-reflection profile BSS–66 (collected in 2011 on survey B–05–11–CC), which crosses shelf west of Ragged Point; see Map A for location. Dashed red lines show faults, including west strand of San Gregorio–Hosgri Fault Zone (SGHF). Magenta symbols show fold axes (diverging arrows, anticline; converging arrows, synclines). Blue shading shows inferred uppermost Pleistocene and Holocene strata, deposited since last sea-level lowstand about 21,000 years ago. Green shading shows Quaternary slope deposits. 'Nu,' undivided Neogene strata; 'KJ,' rocks of the Jurassic and Cretaceous Franciscan Complex. Dashed green lines highlight continuous reflections (not intended to show correlations across faults). Dashed yellow lines are seafloor multiples (echoes of seafloor reflector). Purple triangle shows approximate location of California's State Waters limit (yellow line on Maps A, B, C).

Offshore Shallow Structure and Sediment Distribution, Point Sur to Point Arguello, Central California

By

Samuel Y. Johnson,[1] Stephen R. Hartwell,[1] Janet T. Watt,[1] Jeffrey W. Beeson,[2] and Peter Dartnell[1]

2019

[1] U.S. Geological Survey;
[2] Fugro USA Marine, Inc.

Digital files available at https://doi.org/10.3133/ofr20181158

Suggested Citation: Johnson, S.Y., Hartwell, S.R., Watt, J.T., Beeson, J.W., and Dartnell, P., 2019, Offshore shallow structure and sediment distribution, Point Sur to Point Arguello, central California: U.S. Geological Survey Open-File Report 2018–1158, 3 sheets, scales 1:150,000 and 1:200,000, https://doi.org/10.3133/ofr20181158.

ISSN 2331-1258 (online)
https://doi.org/10.3133/ofr20181158